

ARTICLE

Laser-induced Fluorescence Spectroscopy of NiCl in 12900–15000 cm^{-1}

Cheng-bing Qin, Jian-zheng Zang, Qun Zhang*, Yang Chen*

Hefei National Laboratory for Physical Sciences at the Microscale and Department of Chemical Physics, University of Science and Technology of China, Hefei 230026, China

(Dated: Received on August 22, 2012; Accepted on October 8, 2012)

Laser-induced fluorescence excitation spectra of jet-cooled NiCl molecules were recorded in the energy range of 12900–15000 cm^{-1} . Six vibronic bands with rotational structure have been observed and assigned to the $[13.0]^2\Pi_{3/2}(v'=0-5)-X^2\Pi_{3/2}(v''=0)$ transition progression. The relevant rotational constants, significant isotopic shifts, and (equilibrium) molecular parameters have been determined. In addition, the lifetimes of the observed bands have also been measured.

Key words: NiCl, Laser-induced fluorescence, Isotopic shift

I. INTRODUCTION

Transition metal containing molecules play an important role in many fields, such as astrophysics [1], catalysis [2], materials science [3], and high temperature chemistry [4]. They have been extensively studied both experimentally [5–7] and theoretically [8–11] in the past decades. Among others, the 3d diatomic metal halides are of particular interest, since information of their electronic structure is believed to be instructive for other large systems that contain heavier transition metals.

Spectroscopy of nickel monochloride, NiCl, has been well studied in the visible region, in which a large amount of vibronic bands have been observed and assigned [12–16]. More recent attempts have been made to gain insight into the low-lying electronic states as well as the near-infrared to visible electronic transitions of NiCl, with about 17 electronic states being identified [17–30].

The pure rotational spectrum of NiCl was observed and analyzed by Yamazaki *et al.* in the millimeter and submillimeter-wave region, from which spectroscopic constants of the $X^2\Pi_{3/2}$ ground state were determined [17]. Bernath group has identified several other nearby electronic states including the $A^2\Delta_{5/2}(157.7 \text{ cm}^{-1})$, $X^2\Pi_{1/2}(385.606 \text{ cm}^{-1})$, $A^2\Delta_{3/2}(1645.834 \text{ cm}^{-1})$, and $B^2\Sigma^+(1768.070 \text{ cm}^{-1})$ states by means of laser-induced fluorescence (LIF) and Fourier transform (FT) emission spectroscopy [18–20]. O'Brien group further analyzed these low-lying states via FT emission spectroscopy and intracavity laser absorption spectroscopy (ILS) [21–23]. Very recently, single vibronic levels (SVL) emission spectroscopy has also been used by Reid

group [24] to probe the ground and the nearby low-lying states that all correlate with an electronic configuration of $\text{Ni}^+(3d^9)\text{Cl}^-(3p^6)$, yielding a complete set of vibrational parameters for these states.

The FT and ILS investigations on the near-infrared weak transitions by O'Brien group [21–23, 25–27] have revealed the existence of four electronically excited states, *i.e.*, the $\Omega=3/2$ (9101.26 cm^{-1}), $^4\Phi_{7/2}(10327.356 \text{ cm}^{-1})$, $^2\Sigma^+(12273.18 \text{ cm}^{-1})$, and $^2\Pi_{3/2}(12978.0 \text{ cm}^{-1})$ states, with the relevant molecular constants being derived from the rotational analysis. Other two excited states at around 15000 cm^{-1} , *i.e.*, the $^2\Pi_{3/2}(14977.017 \text{ cm}^{-1})$ and $^2\Delta_{5/2}(14992.74 \text{ cm}^{-1})$ states have been identified via LIF spectroscopy [28], yielding the relevant molecular constants for the four isotopologues of NiCl; in the meantime, an additional weaker transition band (labeled (2, 0) band) has also been recorded [28]. In the $20000\text{--}26000 \text{ cm}^{-1}$ region, Bernath group reported five excited states, *i.e.*, the $\Omega=3/2$ ($21608.625 \text{ cm}^{-1}$), $^2\Delta_{5/2}(21919.90 \text{ cm}^{-1})$, $^2\Delta_{3/2}(22634.432 \text{ cm}^{-1})$, $^2\Pi_{3/2}(24490.594 \text{ cm}^{-1})$, and $^2\Pi_{1/2}(24975.136 \text{ cm}^{-1})$ states [18–20].

Although a considerable amount of spectroscopic investigations of NiCl in the near-infrared and visible regions have been documented so far, most of them except the LIF one [28] utilized high-temperature sources to produce the target NiCl molecules. This inevitably makes it hard, if not impossible, to obtain spectroscopic information on the relatively high vibronic levels and the isotopic-shift effect of interest. In this work we present the LIF excitation spectrum of jet-cooled NiCl recorded in the $12900\text{--}15000 \text{ cm}^{-1}$ region. Six vibronic transition bands, two of which are newly observed, have been analyzed with the rotational constants as well as the significant isotopic shifts being determined. Furthermore, the lifetimes of the observed bands have been measured.

*Authors to whom correspondence should be addressed. E-mail: qunzh@ustc.edu.cn, yangchen@ustc.edu.cn

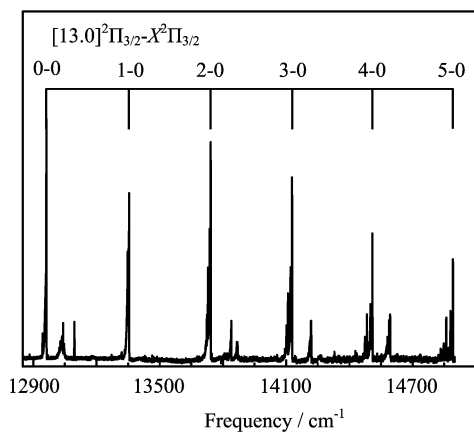


FIG. 1 The survey LIF excitation spectrum of NiCl. Six observed vibronic bands assigned to the $[13.0]^2\Pi_{3/2}-X^2\Pi_{3/2}(v'=0-5)-X^2\Pi_{3/2}(v''=0)$ transitions are indicated by ticks.

II. EXPERIMENTS

The description of our LIF apparatus can be found elsewhere [6]. Briefly, the NiCl molecules were produced, under a pulsed DC discharge condition, by reaction of CH_2Cl_2 molecules with the nickel atoms sputtered from a pair of sharp-head pin electrodes made of pure nickel metal. The CH_2Cl_2 sample gas seeded in argon ($\sim 2\%$) at a stagnation pressure of ~ 500 kPa passed through a pulsed nozzle (General Valve Co., orifice diameter 0.5 mm) into the vacuum chamber. The nickel pins used for DC discharging the mixed $\text{CH}_2\text{Cl}_2/\text{Ar}$ gas was fixed in a Teflon disk with an about 1.5-mm spacing and positioned at ~ 2 mm downstream from the nozzle. The background pressure of the vacuum chamber was ~ 30 and ~ 0.4 mPa, with and without operation of the free jet, respectively.

A Nd:YAG (Spectra Physics, GCR-190, repetition rate of 10 Hz) pumped tunable dye laser (Sirah, PRSC-LG-18) was used to excite the jet-cooled NiCl molecules. To cover the $12900\text{--}15000\text{ cm}^{-1}$ region, the LDS721, LDS698, and DCM dyes were used. The output of the pulsed dye laser (line width $\sim 0.08\text{ cm}^{-1}$, pulse duration ~ 8 ns) was introduced into the vacuum chamber and crossed the jet flow perpendicularly at ~ 4 cm downstream from the point of DC discharge.

The LIF excitation spectra were recorded by monitoring the total fluorescence from the NiCl molecules. The fluorescence signal was collected by a photomultiplier tube (Hamamatsu, CR105) and digitized by an A/D card interfaced to an acquisition computer. No attempt was made to normalize the spectral intensity against the laser power. For lifetime measurements, a digital oscilloscope (Tektronix, TDS3032B) was used to record the fluorescence signal averaged over 128 laser shots. The relative time delays among the nozzle, the laser, and the discharge were controlled by a home-made pulsed multichannel delay generator. Laser wavelength

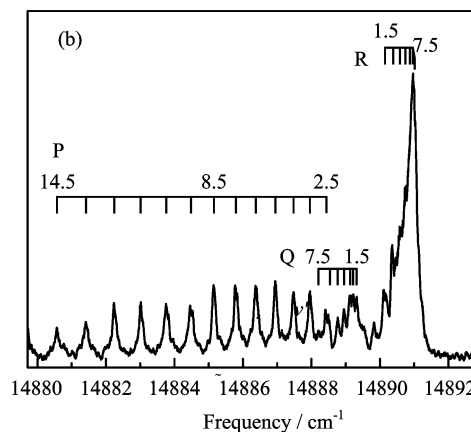
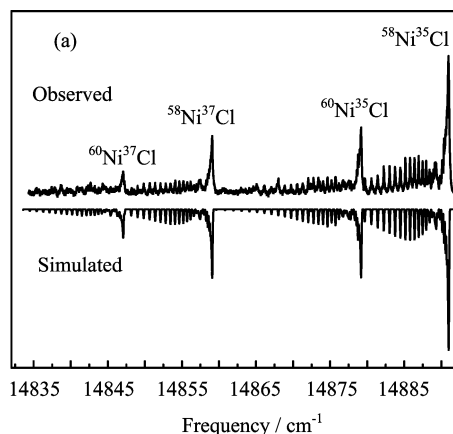


FIG. 2 (a) Rotationally resolved LIF excitation spectrum of the $[13.0]^2\Pi_{3/2}-X^2\Pi_{3/2}(5, 0)$ band of NiCl. The upper (lower) trace is the observed (simulated) spectrum. The subband heads of the four NiCl isotopologue ($^{58}\text{Ni}^{35}\text{Cl}$, $^{60}\text{Ni}^{35}\text{Cl}$, $^{58}\text{Ni}^{37}\text{Cl}$, and $^{60}\text{Ni}^{37}\text{Cl}$) are labeled. (b) Rotational assignments of $^{58}\text{Ni}^{35}\text{Cl}$ are indicated.

was calibrated by a wavemeter (Coherent, WaveMaster 33-2650, resolution $\sim 0.016\text{ cm}^{-1}$).

III. RESULTS AND DISCUSSION

Figure 1 shows the survey LIF excitation spectrum of NiCl recorded. Due to an $\sim 60\text{-}\mu\text{s}$ expansion from the discharge zone to the detection zone, the NiCl molecules under investigation were well cooled down and vastly populated in their ground state. The spectral features of the six observed bands turn out to resemble each other. The two most abundant (among the five naturally occurring) isotopes of nickel are ^{58}Ni (68.08%) and ^{60}Ni (26.22%). For chlorine, ^{35}Cl and ^{37}Cl take 75.78% and 22.24%, respectively. The spectral features associated with the four isotopologues ($^{58}\text{Ni}^{35}\text{Cl}$, $^{60}\text{Ni}^{35}\text{Cl}$, $^{58}\text{Ni}^{37}\text{Cl}$, and $^{60}\text{Ni}^{37}\text{Cl}$) can be readily identified in Fig.2, which displays an exemplified rotational spectrum. The isotopic shifts relate to the upper/lower-

TABLE I Observed isotopic shifts (Obs.) and the differences between observed and calculated values (Obs.–Cal.). Obs. = $T_v(^{58}\text{Ni}^{35}\text{Cl}) - T_v(^{60}\text{Ni}^{35}\text{Cl}, ^{58}\text{Ni}^{37}\text{Cl}, ^{60}\text{Ni}^{37}\text{Cl})$.

(v', v'')	$^{60}\text{Ni}^{35}\text{Cl}$		$^{58}\text{Ni}^{37}\text{Cl}$		$^{60}\text{Ni}^{37}\text{Cl}$	
	Obs./ cm^{-1}	(Obs.–Cal.)/ cm^{-1}	Obs./ cm^{-1}	(Obs.–Cal.)/ cm^{-1}	Obs./ cm^{-1}	(Obs.–Cal.)/ cm^{-1}
(0, 0)	0	0.100	0	0.276	0	0.379
(1, 0)	2.162	–0.181	6.193	–0.139	8.262	–0.454
(2, 0)	4.646	–0.105	12.920	0.076	17.427	–0.254
(3, 0)	7.161	0.036	19.365	0.095	26.607	0.093
(4, 0)	9.511	0.048	25.624	0.042	35.317	0.101
(5, 0)	11.786	0.020	31.846	0.039	43.839	0.052

TABLE II Spectroscopic constants for the $[13.0]^2\Pi_{3/3}-X^2\Pi_{3/2}$ transition bands of NiCl.

v'	$^{58}\text{Ni}^{35}\text{Cl}$		$^{60}\text{Ni}^{35}\text{Cl}$		$^{58}\text{Ni}^{37}\text{Cl}$		$^{60}\text{Ni}^{35}\text{Cl}$	
	T_v/cm^{-1}	B_v/cm^{-1}	T_v/cm^{-1}	B_v/cm^{-1}	T_v/cm^{-1}	B_v/cm^{-1}	T_v/cm^{-1}	B_v/cm^{-1}
0	12959.447(6)	0.16758(3)						
1	13350.397(25)	0.16739(20)	13348.235(26)	0.16350(26)	13344.204(60)	0.16007(64)	13342.135(15)	0.15673(19)
2	13739.850(16)	0.16533(16)	13735.204(25)	0.16278(21)	13726.930(11)	0.15966(11)	13722.423(19)	0.15640(16)
3	14126.140(2)	0.16490(5)	14118.979(10)	0.16271(10)	14106.784(9)	0.15932(22)	14099.533(16)	0.15680(27)
4	14509.182(10)	0.16333(7)	14499.671(8)	0.16160(12)	14483.558(7)	0.15780(7)	14473.865(19)	0.15641(18)
5	14889.389(4)	0.16313(3)	14877.603(6)	0.16104(5)	14857.543(5)	0.15769(4)	14845.550(9)	0.15570(8)

state vibrational parameters through the equation

$$\Delta\nu = (1 - \rho)\omega'_e \left(v' + \frac{1}{2} \right) - (1 - \rho^2)\omega_e\chi'_e \left(v' + \frac{1}{2} \right)^2 - \left[(1 - \rho)\omega''_e \left(v'' + \frac{1}{2} \right) - (1 - \rho^2) \cdot \omega_e\chi''_e \left(v'' + \frac{1}{2} \right)^2 \right] \quad (1)$$

where $\Delta\nu$ denotes the isotopic shift between $^{58}\text{Ni}^{35}\text{Cl}$ and the other three isotopologues; ρ^2 is the ratio of the reduced mass, *i.e.*, μ/μ^* (μ and μ^* being the reduced mass of $^{58}\text{Ni}^{35}\text{Cl}$ and the other three isotopologues, respectively); v' and v'' are the vibrational quantum number of the excited and ground states; ω'_e , ω''_e and $\omega_e\chi'_e$, $\omega_e\chi''_e$ the vibrational constants of the $^{58}\text{Ni}^{35}\text{Cl}$ isotopologue for the excited, ground states. Based on the documented vibrational constants [24, 26], v' and v'' values can be determined with the aid of the observed isotopic shifts in comparison with the calculated values using Eq.(1). The results are listed in Table I. Based on this isotopic-shift analysis, the six predominant spectral features shown in Fig.1 can be unambiguously assigned to the vibronic (5-0, 0) bands of the $[13.0]^2\Pi_{3/2}-X^2\Pi_{3/2}$ transition progression. The band-heads given in our assignment agree well with those reported by O'Brien group [26].

As an example, Fig.2 shows the rotationally resolved LIF excitation spectrum (observed *vs.* simulated) of the (5, 0) band. Note that the observed bands except the (0, 0) band possess a well-separated, four-subband rotational structure in common, with relative intensities

being strong for one, equally middle for two, and weak for the rest one. Obviously, the appearance of such four subbands can only be interpreted as being a result of the isotopic shifts among the four NiCl isotopologues. As expected, the ratios of the relative intensities for those bands coincide with the natural abundance ratios of the four predominant NiCl isotopologues, *i.e.*, $^{58}\text{Ni}^{35}\text{Cl}$: $^{60}\text{Ni}^{35}\text{Cl}$: $^{58}\text{Ni}^{37}\text{Cl}$: $^{60}\text{Ni}^{37}\text{Cl}$ \approx 7.8:2.6:3.0:1.0. For the (0, 0) band, because of a severe spectral congestion of the four subbands as a result of a rather small isotopic shift, we can only give the molecular parameters for the main $^{58}\text{Ni}^{35}\text{Cl}$ isotopologue. Using the molecular parameters reported in Refs.[17, 26], the rotational assignment for this band can be obtained.

Once the vibrational and rotational assignments of all the bands were determined, a set of molecular constants can be obtained through a least-squares fitting procedure. The energy terms were modeled using the expression

$$F(J) = T_v + B_v[J(J+1)] - D_v[J(J+1)]^2 \quad (2)$$

where T_v is the band origin, B_v the rotational constant, and D_v is the centrifugal distortion. The parameters for the ground state were taken from Ref.[17] and held fixed in our simulation. The D_v value for the excited states was fixed at $2.13 \times 10^{-7} \text{ cm}^{-1}$, which was derived from the analysis of the (5, 0) band for the $^{58}\text{Ni}^{35}\text{Cl}$ isotopologue. The least-squares fit was accomplished by the PGOPHER program [30]. The obtained molecular parameters are listed in Table II.

The equilibrium spectroscopic constants for the $[13.0]^2\Pi_{3/2}$ state, such as the electronic state energy

TABLE III Equilibrium parameters for the $[13.0]^2\Pi_{3/2}$ state of NiCl.

		T_0/cm^{-1}	ω_e/cm^{-1}	$\omega_e\chi_e'/\text{cm}^{-1}$	B_e/cm^{-1}	$\alpha_e/10^{-4}\text{cm}^{-1}$	$r_e/\text{\AA}$
$[13.0]^2\Pi_{3/2}$	$^{58}\text{Ni}^{35}\text{Cl}$	12975.49(49)	394.57(38)	1.42(6)	0.16828(40)	9.9(11)	2.143
	$^{60}\text{Ni}^{35}\text{Cl}$	12976.77(35)	392.19(27)	1.42(4)	0.16446(30)	6.1(8)	2.154
	$^{58}\text{Ni}^{37}\text{Cl}$	12978.89(29)	387.99(23)	1.39(4)	0.16122(44)	6.6(11)	2.153
	$^{60}\text{Ni}^{37}\text{Cl}$	12980.17(14)	385.67(11)	1.41(2)	0.15713(40)	2.1(11)	2.166
$[13.0]^2\Pi_{3/2}$ [26]		12978.0(12)	394.22(83)	1.38(18)			
$X^2\Pi_{3/2}$ [24]			427.4(18)	1.8(5)			

term T_e , the vibrational frequency ω'_e , and the vibrational anharmonicity constant $\omega_e\chi'_e$, were calculated by the equation

$$\nu(v', v'') = T_e + \omega'_e \left(v' + \frac{1}{2} \right) - \omega_e\chi'_e \left(v' + \frac{1}{2} \right)^2 - \left[\omega''_e \left(v'' + \frac{1}{2} \right) - \omega_e\chi''_e \left(v'' + \frac{1}{2} \right)^2 \right] \quad (3)$$

and the B_e and α_e values by

$$B_v = B_e + \left(v + \frac{1}{2} \right) \alpha_e \quad (4)$$

The obtained equilibrium constants are given in Table III. The theoretical isotopic shifts can be determined from Eq.(1) by using these equilibrium parameters, when the ground-state constants taken from Ref.[24] were held fixed. The results are listed in Table I.

Furthermore, the lifetimes for the different vibrational levels of the excited state were measured by recording the fluorescence signal decay traces as a function of delay time. The decay signal was averaged over 128 laser pulses at the selected wavelength. A typical decay trace of the fluorescence resulting from the (2, 0) band of the $[13.0]^2\Pi_{3/2}-X^2\Pi_{3/2}$ transition progression of $^{58}\text{Ni}^{35}\text{Cl}$ is displayed in Fig.3. Considering that the NiCl molecules were produced in a very low concentration under a supersonic jet condition in our experiments and hence the expansion of those molecules is reasonably close to a collision-free process, the lifetime of the excited state can be derived from an exponential fit of the fluorescence decay traces. The obtained lifetimes are on approximately the same time scale ($\sim 1.5 \mu\text{s}$) for different vibrational levels and isotopologues, which may provide complementary information about this excited state of NiCl.

IV. CONCLUSION

The jet-cooled laser-induced fluorescence excitation spectrum of NiCl has been recorded in the energy range of 12900–15000 cm^{-1} . Six vibronic bands of the $[13.0]^2\Pi_{3/2}-X^2\Pi_{3/2}$ transition progression were rotationally analyzed for the four NiCl isotopologues. The

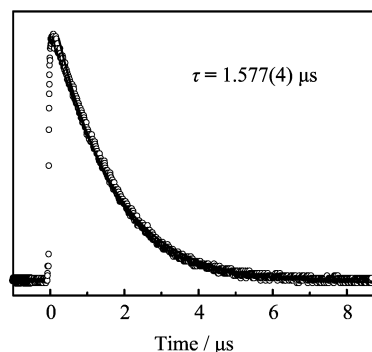


FIG. 3 A typical fluorescence decay trace recorded for the (2, 0) band of the $[13.0]^2\Pi_{3/2}-X^2\Pi_{3/2}$ transition progression. The solid curve is an exponential fit of the decay trace.

molecular parameters and isotopic shifts of the upper state were determined. In addition, the lifetimes of the observed bands were measured under the collision-free condition.

V. ACKNOWLEDGEMENTS

This work was supported by the National Natural Science Foundation of China (No.21273212, No.20873133, and No.21173205), the National Key Basic Research Program of China (No.2010CB923302), the Chinese Academy of Sciences (No.KJCX2-YW-N24), the FR-FCUC (No.WK2340000012), and the USTC-NSRL Joint Funds (No.KY2340000021).

- [1] H. Spinrad and R. F. Wing, *Annu. Rev. Astron. Astrophys.* **7**, 249 (1969).
- [2] G. D. Cody, *Annu. Rev. Earth. Planet. Sci.* **32**, 569 (2004).
- [3] C. W. Bauschlicher and P. Maitre Jr., *Theor. Chim. Acta.* **90**, 189 (1995).
- [4] A. J. Merer, *Annu. Rev. Phys. Chem.* **40**, 407 (1989).
- [5] T. C. Steimle, *Int. Rev. Phys. Chem.* **19**, 455 (2000).
- [6] S. Zhang, J. Zhen, Q. Zhang, and Y. Chen, *J. Mol. Spectrosc.* **252**, 77 (2008).
- [7] C. J. Evans and M. C. L. Gerry, *J. Am. Chem. Soc.* **122**, 1560 (2000).

- [8] K. Balasubramanian, *J. Chem. Phys.* **93**, 8061 (1990).
- [9] A. J. Bridgeman and J. Rothery, *J. Chem. Soc., Dalton Trans.* 211 (2000).
- [10] B. Liang and L. Andrerws, *J. Phys. Chem. A* **106**, 6295 (2002).
- [11] B. Liang and L. Andrerws, *J. Phys. Chem. A* **106**, 6945 (2002).
- [12] K. R. More, *Phys. Rev.* **54**, 122 (1938).
- [13] S. P. Reddy and P. T. Rao, *Proc. Phys. Soc.* **75**, 275 (1960).
- [14] S. V. K. Rao, S. P. Reddy, and P. T. Rao, *Z. Physik.* **166**, 261 (1962).
- [15] R. Gopal, *Curr. Sci.* **50**, 854 (1981).
- [16] C. V. Reddy, A. L. Narayana, and P. T. Rao, *Acta Phys. Hung.* **63**, 295 (1988).
- [17] E. Yamazaki, T. Okabayashi, and M. Tanimoto, *Astrophysical J.* **551**, L199 (2001).
- [18] T. Hirao, C. Dufour, B. Pinchemel, and P. F. Bernath, *J. Mol. Spectrosc.* **202**, 53 (2000).
- [19] A. Poclet, Y. Krouti, T. Hirao, B. Pinchemel, and P. F. Bernath, *J. Mol. Spectrosc.* **204**, 125 (2000).
- [20] Y. Krouti, A. Poclet, T. Hirao, B. Pinchemel, and P. F. Bernath, *J. Mol. Spectrosc.* **210**, 41 (2001).
- [21] C. A. Rice and L. C. O'Brien, *J. Mol. Spectrosc.* **221**, 131 (2003).
- [22] C. A. Rice, T. L. Kellerman, B. Owen, L. C. O'Brien, H. Cao, and J. J. O'Brien, *J. Mol. Spectrosc.* **235**, 271 (2006).
- [23] K. D. Gibbs, D. J. Trader, L. C. O'Brien, and J. J. O'Brien, *J. Mol. Spectrosc.* **240**, 64 (2006).
- [24] L. G. Muzangwa, V. L. Ayles, S. Nyambo, and S. A. Reid, *J. Mol. Spectrosc.* **269**, 36 (2011).
- [25] L. C. O'Brien, K. M. Homann, T. L. Kellerman, and J. J. O'Brien, *J. Mol. Spectrosc.* **211**, 93 (2002).
- [26] J. J. O'Brien, J. S. Miller, and L. C. O'Brien, *J. Mol. Spectrosc.* **211**, 248 (2002).
- [27] S. Tunturk, L. C. O'Brien, and J. J. O'Brien, *J. Mol. Spectrosc.* **225**, 225 (2004).
- [28] J. W. H. Leung, J. Ye, A. S. C. Cheung, K. D. Gibbs, D. L. Palmer, L. C. O'Brien, and J. J. O'Brien, *J. Mol. Spectrosc.* **238**, 42 (2006).
- [29] W. Zou and W. Liu, *J. Chem. Phys.* **124**, 154312 (2006).
- [30] C. M. Western, *PGOPHER: A Program for Simulating Rotational Structure*, University of Birstol, <http://pgopher.chm.bris.ac.uk>.